Time electromagnetic response of a controlled regular wavefield in a wave basin for a monostatic configuration

Ahmad Gharib, Raphaël Renoud, Christophe Bourlier, Nicole de Beaucoudre, Félicien Bonnefoy

Time electromagnetic response of a controlled regular wave field in a wave basin for a monostatic configuration

Ahmad Gharib[1], François Poulain[1], Christophe Bourlier[1], Nicole de Beaucoudrey[1],
Félicien Bonnefoy[2], Laurent Davoust[2].
[1]IREENA, Fédération CNRS Atlanstic, Université de Nantes, Polytech'Nantes, La Chantrerie, BP 50609, 44306 Nantes
[2]Laboratoire de Mécanique des Fluides, CNRS, Ecole Centrale de Nantes, 1 rue de la Noé, BP 92101, 44321 Nantes
ahmad.gharib@univ-nantes.fr

***Abstract*- In this paper, the microwave signal backscattered by a controlled swell in a wave basin is studied, as a function of time, both theoretically and experimentally. The electromagnetic response of a surface depends on its shape, its dielectric characteristics, and antennas characteristics and positions. Measurements acquired with a monostatic microwave scatterometer installed above a wave tank, in which regular waves are generated, are compared with simulation results obtained by two electromagnetic models, based on the Physical Optics approximation (PO) and the Method of Moments (MoM).**

I. INTRODUCTION

The study of electromagnetic waves scattered by sea surfaces has many applications: target detection within sea clutter, oil spills detection…

The radar must be able to detect the presence of an object above the sea surface. Thus, to know the contribution of the sea clutter in radar echoes, electromagnetic scattering models must be developed. Depending on the application, these models are either asymptotic, to obtain fast results, or rigorous, to validate the first ones. In addition, it is also interesting to compare simulations with measurements.

Nevertheless, a direct comparison of any scattering model with experimental data often remains a difficult task, because parameters characterizing the sea surface are not accurately known. Thus it is very interesting to implement a scatterometer to determine the Radar Cross Section (RCS) of a controlled swell generated in a wave tank. Currently, this work is done in collaboration with the LMF (Fluid Mechanics Laboratory) of the ECN (Ecole Centrale de Nantes) located in Nantes, France.

In this paper, measurements obtained from this scatterometer are compared with asymptotic and rigorous theoretical results. Firstly, to simplify this difficult problem, regular surfaces are considered (one-dimensional surfaces).

The electromagnetic response of a swell generated in the wave tank is calculated. Simulations will use hydrodynamic models of the water surface coupled with electromagnetic models deriving the surface RCS, as well as radiation patterns of antennas.

In section II, we briefly describe the experimentation, which is a part of the DIMBAHO (DIffusiomètre Microonde sur BAssin de HOule or "Microwaves Scatterometer on a wave tank") project [1, 2].

In section III, two scattering models are presented. The first one is based on an asymptotic fast method, the physical optics approximation [3]; the second one is based on a rigorous method, the Method of Moments [4, 5]. The last section presents comparisons between theoretical models and experimental data.

II. EXPERIMENTAL SETUP

The wave basin is a rectangular pool (length: 50 m, width: 30 m, depth: 5 m) of fresh water. Paddles located on one side of the basin are controlled by sequence in order to generate either regular or irregular wavefields. Generated regular waves are characterized by a wave height, defined as the peak-to-trough distance (2A), ranging from 5 cm to 30 cm and a wavelength (L) chosen here equal to either 6.24 m or 3.14 m.

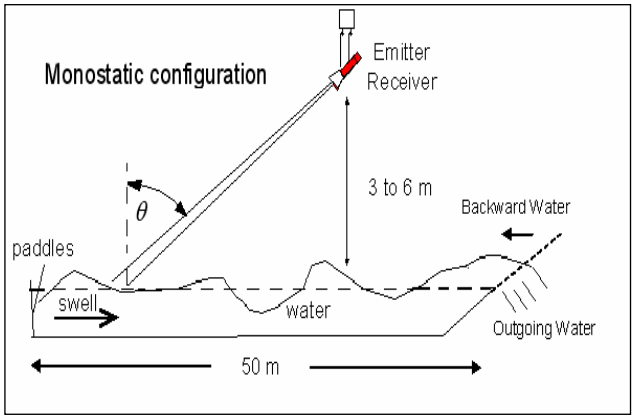

Fig.1 Transversal view of the experimental configuration

While the wavemaker is activated, we observe that the water surface is not smooth. On top of the desired long waves (3-6 m wavelength), we note the propagation of short ripples (5-20 cm wavelength). Those ripples are generated both by the gaps existing between the wavemaker paddles and at the beach located at the end of the wave tank, where waves break

in order to avoid reflection (see Fig. 1). The emitter-receiver device (monostatic configuration) is composed of two horn antennas with rectangular apertures. Due to the ceiling, the distance from antennas to the mean water surface can reach a maximum height of 6 meters. Antennas inclinations can reach 40°. The polarization is VV or HH and the scatterometer electromagnetic frequency ranges from 8 to 12 GHz. Antennas are connected to an analyzer driven by a computer. The sampling time of measurements is 0.05 second.

III. SCATTERING MODELS

A. *Scattering models*

The 2D problem consists in solving the equation of the scattered field (Fig. 2) given by:

$$\psi_s(\vec{r}') = \int_S \left[\psi(\vec{r}) \frac{\partial g(\vec{r},\vec{r}')}{\partial n} - g(\vec{r},\vec{r}') \frac{\partial \psi(\vec{r})}{\partial n} \right] dS \qquad (1)$$

The variables $\psi(\vec{r})$ and $\partial\psi(\vec{r})/\partial n$ are respectively the total field and its derivative with respect to the normal to the surface on the surface, g is the scalar Green function in the upper medium denoted as Ω_0. The vectors $\vec{r}$ and $\vec{r}'$ stand for the coordinates of a point on and above the surface, respectively.

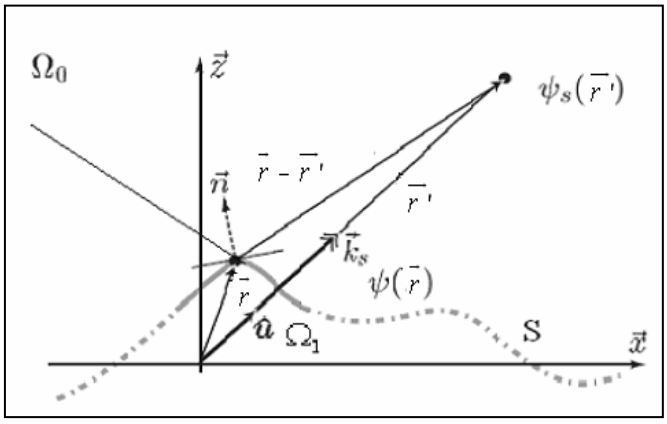

Fig2. Scattered field by a rough surface

To solve the problem, we must know $\psi(\vec{r})$ and $\partial\psi(\vec{r})/\partial n$. The two unknowns verify the following integral equations:

$$\psi_i(\vec{r}') = -\int_S \left[\psi(\vec{r}) \frac{\partial g(\vec{r},\vec{r}')}{\partial n} - g(\vec{r},\vec{r}') \frac{\partial \psi(\vec{r})}{\partial n} \right] dS \qquad (2)$$

$$0 = \int_S \left[\psi(\vec{r}) \frac{\partial g_1(\vec{r},\vec{r}')}{\partial n} - \rho_{01} g_1(\vec{r},\vec{r}') \frac{\partial \psi(\vec{r})}{\partial n} \right] dS \qquad (3)$$

Where, ψ_i is the incident field on the surface, $\rho_{01} = \varepsilon_1 / \varepsilon_0$ for the V polarization and $\rho_{01} = 1$ for the H polarization, ε_0 is the permittivity in the upper medium (Ω_0), ε_1 and g_1 are the permittivity and the scalar Green function in the lower medium Ω_1 (Fig. 2).

In order to model the electromagnetic field scattered by a rough surface, the Physical Optics (PO) approximation and the Method of Moments (MoM) are applied. The PO approach allows a fast computation of the scattered electromagnetic field, but it requires simplifying hypothesis. To verify the validity of this method in our application, we compare it with the rigorous MoM, which demands more extensive computing time and memory space.

The first method to calculate $\psi(\vec{r})$ and $\partial\psi(\vec{r})/\partial n$ is the PO approximation. This method specifies that $\psi(\vec{r})$ and $\partial\psi(\vec{r})/\partial n$ at a point M ($\vec{r}$) on the surface are supposed to be the same that should exist on its infinite tangent plane. This leads to:

$$\psi_M = \left[1 + R(\theta)\right] \psi_{iM} \qquad (5)$$

$$\frac{\partial \psi_M}{\partial n} = j\vec{k}_i \vec{n} \left[1 - R(\theta)\right] \psi_{iM} \qquad (6)$$

where R is the Fresnel coefficient, θ is the angle between the tangent plane normal $\vec{n}$ and the incident wave vector $\vec{k}_i$ and ψ_{iM} is the incident wave.

The PO is valid if the condition $\rho\cos^3(\theta) >> \lambda$ [6] is satisfied, where ρ is the radius of curvature of the surface, θ is the local incident angle and λ is the Radar wavelength that is equal to 3 cm (f=10 GHz).

The second method presented in this paper is the MoM. It is appropriate for homogenous media and it is based on the discretization of integral equations. In addition, using point matching and pulse basis functions, a linear system is obtained, which requires the inversion of an impedance matrix. For more details, see for instance the textbook of Tsang et al. [7]. For a small size matrix, a LU inversion technique can be applied. For large problems, the fast methods, such as the FB-SA (Forward-Backward Spectral-Acceleration) [8] or the BMIA/CAG (Banded Matrix Iterative Approach/Canonical Grid) [9, 10], can be applied.

B. *Description of the regular surface*

The electromagnetic response of both scattering models is estimated on regular wave fields which are computed by a Numerical Wave Tank (NWT) developed at LMF [11, 15]. Such regular waves are generated with a monochromatic wavemaker motion and they are characterized by their amplitude A and spatial period L (wavelength defined as the horizontal distance between two consecutive maxima). According to linear wave theory, the wavelength L of the regular wave is given by:

$$L = \frac{gT^2}{2\pi}, \qquad (7)$$

Where g = 9,81m/sis the gravity constant, T is the time period (Fig. 3).

The two probes S1 and S2 in Fig. 3 measure the water height with a sampling time /dt/ equal to 0.01 s. The distance

between these probes is 10 m. The probe S2 measures the height of the swell under the Radar.

The NWT is based on the resolution of the nonlinear wave generation and propagation equations derived for an irrotationnal flow and inviscid fluid [11, 15]. Those potential flow theory equations are solved numerically by means of a spectral method chosen for its accuracy. The NWT reproduces the main features of the physical basin, including the wavemaker geometry, the reflective side-walls and the beach that absorbs the wave at the end wall. In order to compare with experiments, the motion of the physical wavemaker is directly input in the NWT. The free surface elevation is computed at the probes location. These simulations do not however take into account the propagation of short ripples due to the wave reflections at the end of the wave tank.

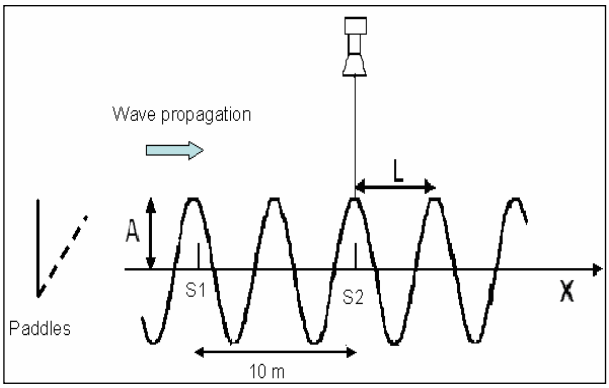

Fig.3 Characteristics of a regular surface.

The frequency (1/T) of the studied surfaces is either 0.5 Hz or 0.7 Hz, and its amplitude A can reach 15 cm. The spatial sampling used for the surface simulations is of the order of several λ. This sampling can be reduced to 0.1λ by using the Spline function to interpolate the measured surface height.

C. Numerical results

The surface, depicted in Fig. 3, is illuminated by the antenna electromagnetic wave. The radar frequency is 10 GHz (λ= 3 cm) and the polarization is VV. First, we focus on analytical calculation of the antenna gain. It can be calculated approximately using an analytical formula [12]. Figs 4 and 5 compare the gain in the E plan with that obtained experimentally. A very good agreement is observed at 10 GHz.

In Figs. 6 and 7, the modulii of the total field and of its normal derivative, derived under the PO and the MoM methods, are plotted versus the surface abscissa. Also, in figure 7 the modulus of the field scattered by the surface is plotted versus the scattering angle. The amplitude of the surface (maximum height measured by S2) is A = 15 cm = 3λ, and its period T = 2s (L = 6.25 m = 208.2 λ). The length surface is then = 1.92 L = 12 m, the antennas inclination θ_i= 0. For the MoM, the sampling step on the surface is 0.1λ implying 4001 samples and 8002 unknowns since the surface is dielectric (complex permittivity ε_r=1.3+0.1j).

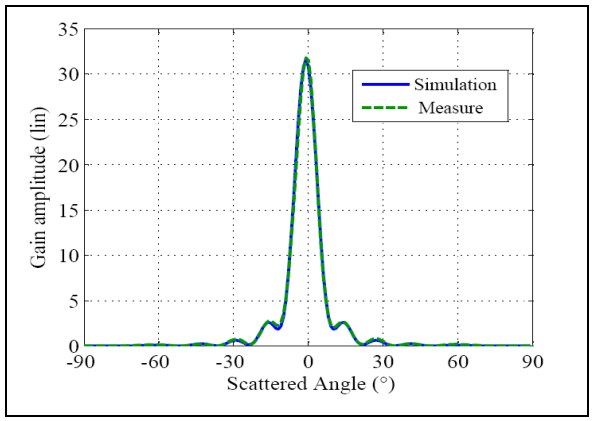

Fig.4 Calculated and measured radiation Patterns in E plan

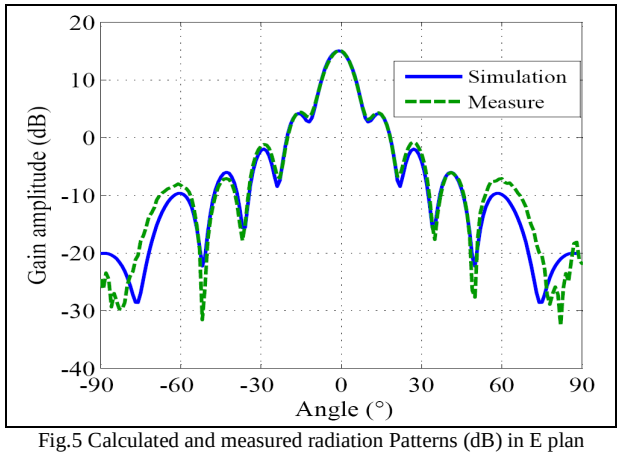

Fig.5 Calculated and measured radiation Patterns (dB) in E plan

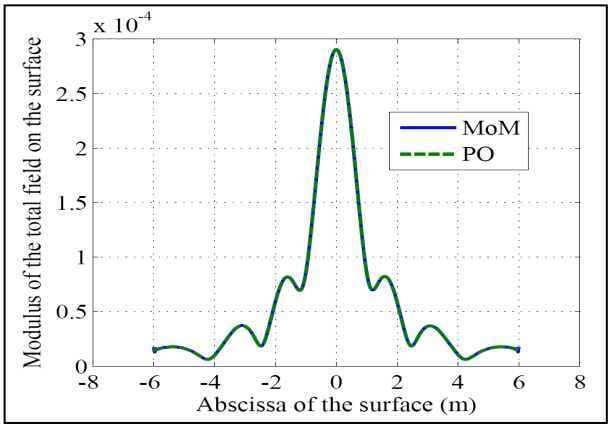

Fig.6 Modulus of the total field on the measured surface: A=15 cm, T=2s, f=10 GHz, θ_i=0°, ε_r=1.3+0.1j, V polarization

Figs 6, 7 and 8 show a very good agreement between the two methods for the measured surface of amplitude A = 15 cm. Also a very good agreement is observed, in other simulations not displayed here, between the two methods for lower amplitudes with the same conditions as for the experiments [13, 14].

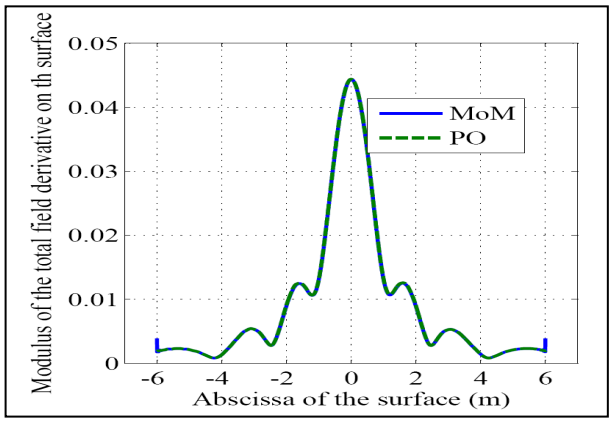

Fig.7 Modulus of the total field derivative on the measured surface: Same parameters as in Fig.6

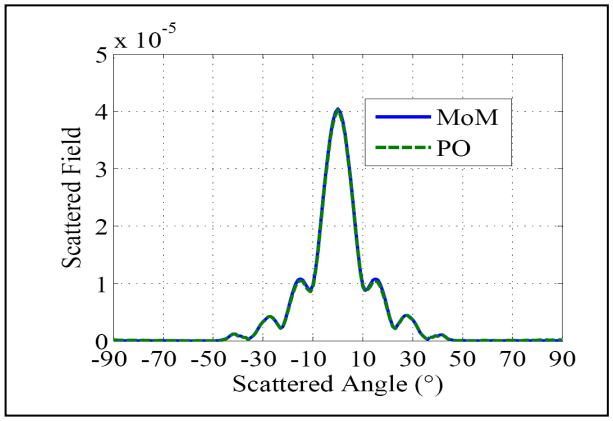

Fig.8 Modulus of the scattered field by the measured surface. Same parameters as in Fig.6.

A good agreement is also observed for other configurations. For example, in figure 9 the electromagnetic scattering field is plotted versus the time for the same surface and for an inclination angle θ_i= 20°. In conclusion, the PO approximation is valid for our application

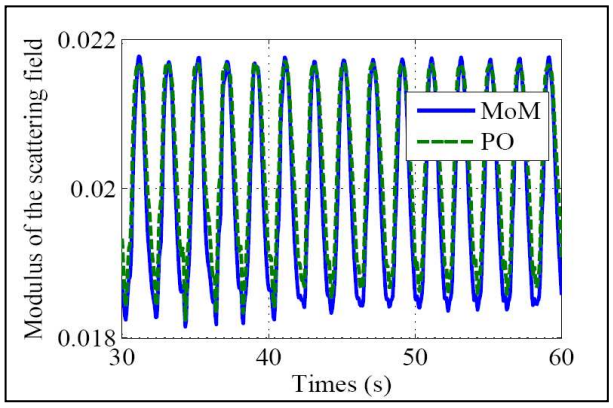

Fig.9 Modulus of the scattered field calculated by PO and MoM in an interval of time. The surface characteristics are same as before, the antennas inclination θ_i= 20°.

IV. Comparison between experiments

To validate the theoretical model, the results calculated by the PO are compared with those obtained from the experimentation. According to the radar equation, the power received by an antenna illuminating a surface of length l is given by:

$$P_r = \frac{\lambda^2}{(4\pi)^3} P_e \int_l \frac{G(l)^2 \sigma(l)}{r(l)^4} dl \qquad (8)$$

P_r : The power received by the antenna,
P_e : The power emitted by the antenna,
λ: The radar wave length (0.03 m),
r : Distance between the antenna and the illuminated surface,
G : Gain of the antenna, calculated and compared below with experimental one.
σ : Scattering coefficient.

The scattering coefficient σ is defined as:

$$\sigma = \lim_{r\to\infty} \frac{2\pi r |\psi_s|^2}{\mathrm{Re}\int \frac{j}{k\cos\theta}\psi(l,0)\frac{\partial\psi(l,0)}{\partial z} dl}, \qquad (9)$$

where,
k : Wave vector,
θ : Local incidence angle,
r : Distance between illuminated surface and antenna,
$\psi(\vec{r})$ and $\partial\psi(\vec{r})/\partial n$ calculated by PO method. Their substitutions in equation (1) allow us to compute the scattered field ψ_s.
$\psi(l,0)$ and $\partial\psi(l,0)/\partial z$ are respectively the field and its derivative on the mean plan of the surface.

In figures 10 and 11, the modulii of the scattered field calculated by the PO method and measured by antennas are plotted versus time, respectively. For the PO, the generated swell is characterized by A = 15 cm and L = 6.25 m. The antennas inclination θ_i = 0° and the antennas frequency f = 10 GHz. Antennas are 6 meters above the mean surface. The sampling time of the antennas is 0.05 seconds.

A good qualitative agreement is observed between theoretical and experimental results. The difference seen on both figures comes from ripples which are not considered in electromagnetic simulations.

Short ripples (5-20 cm wavelength), observed on the basin surface, can be modeled as a summation of sinusoidal surfaces of small amplitudes and high frequencies (3 - 40Hz). These frequencies can be determined by calculating the Fourier Transform of the surface measured by the probe under the radar in versus of the time. The vibration of this probe, moving while it takes measures, creates an additional frequency of 17 Hz.

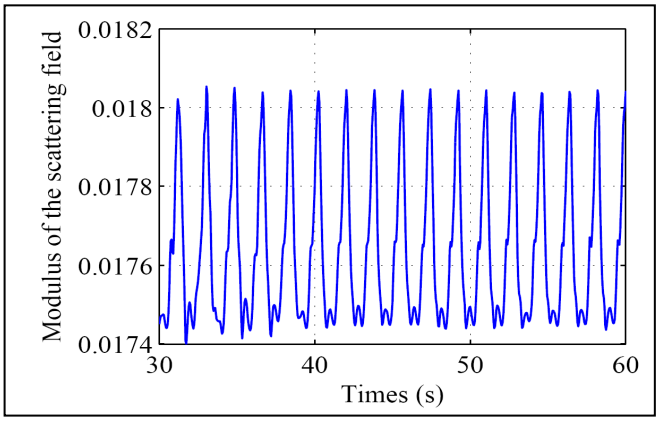

Fig 10. Modulus of the scattering field versus time calculated by PO. Swell amplitude A = 15 cm, swell spatial period L = 6.452 m Antennas inclination $\theta_i = 0°$, Antennas height = 6 m.

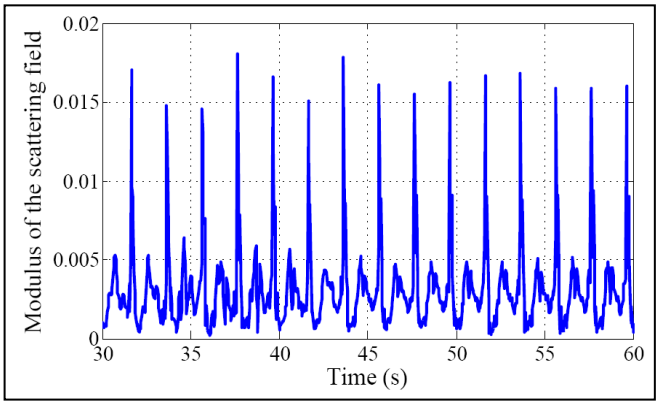

Fig 11. Modulus of the scattered field versus time measured by antennas. Same parameters as in Fig. 10

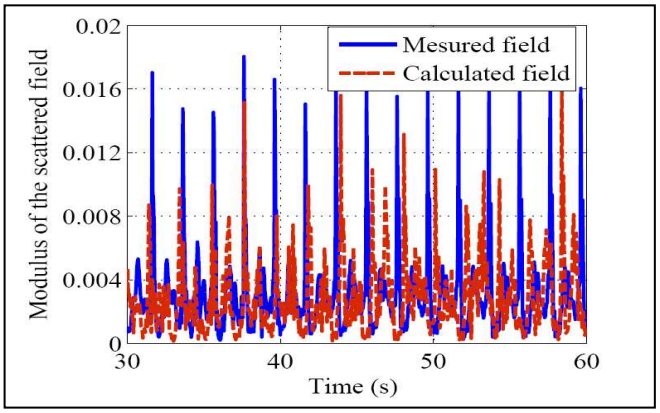

Fig 12. Modulus of the scattered field versus time calculated for a surface with additional ripples (A=0.0025 m; f = 17Hz). Same parameters as Fig. 10.

In Fig.12, measured and calculated scattering fields are plotted versus time, for which, in the generated surface, the ripples effect is modeled as a sinusoidal surface of amplitude A=0.0025m and frequency f=17 Hz (vibration frequency of the probe).

Two levels of maxima are observed for each plot in the figure. The highest, in range of 0.015, correspond to the contribution of swell troughs, and the lowest, in range of 0.005, correspond to the contribution of swell peaks. Also a good qualitative agreement is observed between results for simulated surface, surface with additional ripples and experimental results. Otherwise the modulus of the scattered field in figure a modulus level of the received field in figure 12 is lower than of the figure 10. This is due to additional roughnesses coming from additional ripples.

V. CONCLUSION

In this paper, firstly, the PO approximation was validated from the rigorous MoM for surfaces met in our applications. Indeed, a very good agreement was observed between the scattered fields computed by these two methods. Also, a good qualitative agreement is observed between results computed from the PO and those obtained experimentally.

In order to interpret a more realistic case, the ripples that appear on the surface, due to the reflection of the waves at the end of the wave tank, are modeled as sinusoidal surfaces with small amplitudes and high frequencies. The agreement seems then to be better, as observed in Fig.11.

VI. REFERENCES

[1] F.Poulain, N. de Beaucoudrey, S. Loin, N. Déchamps, J.M. Rousset JNM 2007 : XVes Journées Nationales MicroOndes –Toulouse 23-25 Mai 2007 Diffusiomètre micro-ondes sur bassin de houle: banc de caractérisation monostatique.

[2] F. Poulain, N. de Beaucoudrey, S. Loin, N. Déchamps, J.M. Rousset OCOSS2007 : Innovations dans les techniques pour l'observation des côtes et des océans: senseurs, modélisation et systèmes,, 26-27 juin 2007, Paris, Expérimentation sur bassin de houle d'un diffusiomètre micro-ondes monostatique.

[3] L.Tsang, J.A.Kong and K.H. Ding "Scattering of Electromagnetic Waves in Theories and Applications," John Wiley and Sons, New York, 2001.

[4] F. Harrington. Field Computation by Moments Methods. IEEE Press, Piscataway, NJ, 1993

[5] L. Tsang and J. A. Kong, " Scattering of Electromagnetic Waves in Advances Topics, " John Wiley and Sons, New York, 2001

[6] F.G. Bass and I. M. Fuks, "Wave Scattering from Statistically Rough surfaces," Pergamon press, Paris, 1979.

[7] L. Tsang, J. A. Kong, K.-H. Ding and C. O. AO. Scattering of Electromagnetic Waves: Numerical Simulations, volume 2. Wiley Series on Remote Sensing, 2001.

[8] H.T.Chou and J.T.Johnson, "A novel acceleration algorithm for the computation of scattering from rough surfaces with the forward-backward method," Radio Science, vol.33, 1277-1287, 1998.

[9] L. Tsang, C.H. Chang, H. Sangani, A Ishimaru and P. Phu, "A banded matrix iterative approach to monte carlo simulations of large scale random rough surface scattering: TE case," J.Electromagn. Waves Appllicat. vol 29, no.9, pp. 1185-1200, 1993.

[10] L. Tsang, C. H. Chang, K. Pak and H. Sangani, " Monte- Carlo simulations of large – scale problems of random rough surface scattering and applications to grazing incidence with the BMIA/Canonical Grid Method," IEEE Trans. Ant. Prop., vol. 43, no. 8, pp. 851-859, 1995.

[11] F. Bonnefoy « Modélisation expérimentale et numérique des états de mer complexe » PHD, 31-03-2005

[12] Constantine A. BALANIS. Antenna theory, Analysis and Design, published by Jhon Wiley& Sons, Inc., Hboken, New Jersey 2005

[13] A. Gharib, Christophe Bourlier, François Poulain, Nicole de Beaucoudrey Echo Radar monostatique d'une houle contrôlée. JNM 2009.

[14] A. Gharib, F. Poulain, C. Bourlier, N. de Beaucoudrey, "Contribution of the sea surface in monostatic radar echoes", *International Radar Conference, RADAR'09*, Bordeaux, octobre 2009.

[15] G. Ducrozet, F. Bonnefoy, D. Le Touzé and P. Ferrant.Implementation and Validation of Nonlinear Wave Maker Models in a HOS Numerical Wave Tank. IJOPE, vol. 16, no. 3, pp. 161-167, 2006.